Chemical Engineering Journal 165 (2010) 784–797

Contents lists available at ScienceDirect

Chemical Engineering Journal

journal homepage: www.elsevier.com/locate/cej

Dye sensitized visible light degradation of phenolic compounds

R. Vinu, Sneha Polisetti, Giridhar Madras*

Department of Chemical Engineering, Indian Institute of Science, Bangalore 560012, India

ARTICLE INFO

Article history:
Received 27 July 2010
Received in revised form 1 October 2010
Accepted 9 October 2010

Keywords:
Dye sensitization
Photocatalysis
Visible light
Chlorophenols
Network reduction

ABSTRACT

The present research work reports the eosin Y (EY) and fluorescein (FL) sensitized visible light degradation of phenol, 4-chlorophenol (CP), 2,4-dichlorophenol (DCP) and 2,4,6-trichlorophenol (TCP) using combustion synthesized nano-TiO_2 (CS TiO_2). The rate of degradation of the phenolic compounds was higher in the presence of EY/CS TiO_2 compared to FL/CS TiO_2 system. A detailed mechanism of sensitized degradation was proposed and a mechanistic model for the rate of degradation of the phenolic compound was derived using the pyramidal network reduction technique. It was found that at low initial dye concentrations, the rate of degradation of the phenolic compound is first order in the concentration of the dye, while at high initial dye concentrations, the rate is first order in the concentration of the phenolic compound. The order of degradation of the different phenolic compounds follows: CP > TCP > DCP > phenol. The different phenolic and dye intermediates that were formed during the degradation were identified by liquid chromatography–mass spectrometry (LC–MS) and the most probable pathway of degradation is proposed.

1. Introduction

Solar radiation is the most abundantly available renewable and clean source of energy, which is composed of more than 50% of visible radiation and less than 4% of ultraviolet (UV) radiation [1]. In the UV region, pristine TiO_2 has been the "benchmark photocatalyst" for the degradation of organic compounds, reduction of metal ions, and destruction of microorganisms. However, the wide band gap (3.2 eV) of pristine TiO_2 makes it a poor photocatalyst in the solar/visible region. Some of the modifications of TiO_2 to enable its visible light response include, (i) anion doping to narrow the band gap, and (ii) heterostructuring with other narrow band gap semiconductors or dyes as sensitizers [2]. In this report, we focus on coupling an organic dye with TiO_2 to induce the degradation of phenolic compounds in the presence of visible light.

It is well known that singlet oxygen ($^1O_2(^1\Delta_g)$), formed by the interaction of the triplet state of the dye with molecular oxygen, is the key species involved in the sensitized oxidation of organic compounds in the absence of a heterogeneous photocatalyst [3]. However, in the presence of a semiconductor photocatalyst like TiO_2, the mechanism of sensitization is quite different. The mechanism involves the excitation of the dye from the ground state (D) to the triplet excited state (D*) by the action of a visible light photon ($\lambda > 400$ nm). This excited state dye species is converted to a semioxidized radial cation ($D^{\bullet+}$) by the injection of an electron (e^-) into the conduction band (CB) of TiO_2 [1]. This trapped electron then forms superoxide radical anion ($O_2^{\bullet-}$) by the reaction with dissolved oxygen in the system (Fig. 1), which results in the formation of hydroxyl species ($OH^\bullet$). These $OH^\bullet$ radicals are responsible for the oxidation of the organic compounds. Dye sensitized degradation is primarily driven by good adherence of the dye onto the surface of TiO_2, and the presence of O_2 to scavenge the injected electrons from the conduction band of TiO_2 [4].

Zhang et al. [5] have recently studied the aerobic selective oxidation of alcohols in the presence of an anthraquinonic dye (alizarin red S) sensitized TiO_2, and a nitroxyl radical (2,2,6,6-tetramethylpiperidinyloxyl). The mechanism involves the formation of a dye radical cation, which oxidizes the nitroxyl radical. This oxidized species was found to be responsible for the selective oxidation of alcohols to aldehydes. Yin et al. [6] have shown that the presence of eosin Y (EY) accelerates the degradation of rhodamine B in the presence of P25. Conjugated polymers like poly(aniline) [7] and poly(thiophene) [8] have also been used as sensitizers of TiO_2 for the degradation of dyes. The role of dissolved oxygen and of active species generated by photo-induced reactions in the photocatalytic degradation of phenol was investigated extensively [9]. Although the above studies have elucidated the mechanism of sensitization in terms of electron injection to facilitate the formation of active species, the kinetics of such processes is still obscure due to the presence of the dye and the organic substrate. Furthermore, it is observed that the sensitizing dye also undergoes oxidation and degrades during the reaction. Therefore, a thorough study of the complex interaction of the dye,

* Corresponding author. Tel.: +91 80 22932321; fax: +91 80 23601310.
E-mail addresses: giridhar@chemeng.iisc.ernet.in, giridharmadras@gmail.com (G. Madras).

1385-8947/$ – see front matter © 2010 Elsevier B.V. All rights reserved.
doi:10.1016/j.cej.2010.10.018

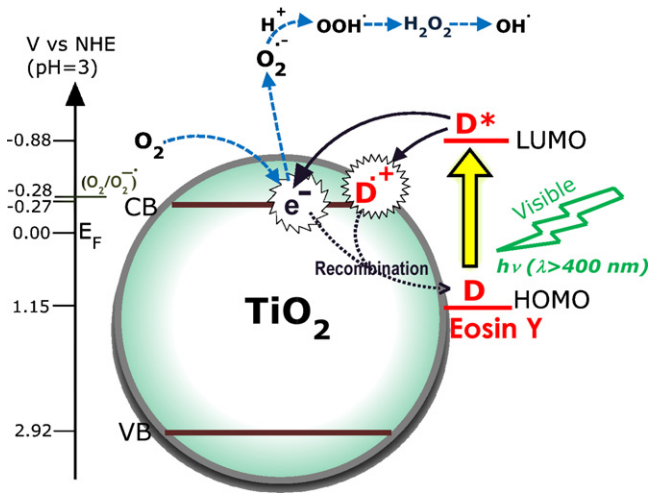

Fig. 1. Mechanism of electron injection from the excited state of EY, and the formation of dye radical cation and superoxide radicals.

organic substrate, and TiO_2 is required to understand the kinetics. In this research work, two xanthene-fluorone dyes, viz., eosin Y (EY) and fluorescein (FL) are employed to sensitize the degradation of substituted phenolic compounds in the presence of combustion synthesized nano-TiO_2 (CS TiO_2). We have shown in our earlier works that CS TiO_2 exhibits higher solar photocatalytic activity compared to the conventional Degussa P-25 TiO_2 (P25) for the degradation of dyes [10].

Cyclic network reduction is a useful method to find the rate of complex reaction networks [11]. Although originally established for homogeneous reactions, the method can also be applied to heterogeneous reactions by assuming pseudo steady state on the intermediate species. Wu and Chern [12] have adopted this technique to derive the rate equation for the photocatalytic degradation of methylene blue. We have also modeled the simultaneous degradation of phenolic compounds and metal ions using dual-cycle network reduction [13], and the sono-photocatalytic degradation of anionic dyes using dual-pathway network reduction techniques [14], respectively. The versatility of this technique has been extended in this work for the dye sensitized degradation of phenolic contaminants. The harmful effects of phenolic contamination in water is well known, as upto 10% of phenol and chlorophenols are widely used as intermediates in the manufacture of chlorinated herbicides and pesticides. Because these organic compounds are toxic, their safe disposal is of primary concern for the environmental remediation.

In the broad scope of waste water remediation, this work is beneficial in two aspects. Firstly, the adsorption of the dye on the surface of TiO_2 catalyst extends the absorption spectrum of TiO_2 to the visible regime. Secondly, the system containing the dye and the phenolic compound represents a classic model of a real effluent stream, which is usually a mixture of different organic compounds, metal ions and surfactants. Thus, this study assumes importance in the effective detoxification of effluent streams containing a dye and a phenolic compound in presence of visible light source. The kinetic model presented in this work will be useful in the photocatalytic reactor models which utilize dye-sensitized degradation.

Therefore, the purpose of this work is fourfold. Firstly, we have shown the superior activity of CS TiO_2 compared to the commercial catalyst, Degussa P-25 TiO_2 (P25) for the EY sensitized degradation of phenol, 4-chlorophenol (CP), 2,4-dichlorophenol (DCP) and 2,4,6-trichlorophenol (TCP). Secondly, based on the experimental observations, we have proposed a pyramidal network mechanism for the sensitized degradation of the phenolic compounds, and have modeled the reaction using network reduction. Thirdly, we have evaluated the rate coefficients of degradation of the phenolic compounds, and rationalized them based on the mechanism of degradation. Finally, we have suggested a possible pathway of degradation by identifying the phenolic and dye intermediates.

2. Experimental

2.1. Materials

The phenolic compounds, viz., phenol (Rankem Chemicals, India), 4-chlorophenol (CP; S.D. Fine Chem., India), 2,4-dichlorophenol (DCP; Spectrochem, India), 2,4,6-trichlorophenol (TCP; Central Drug House, India) and 4-nitrophenol (NP; Spectrochem, India), and the dyes, viz., eosin Y (EY; Color index (C.I.) No. 45380; Merck, India), fluorescein sodium (FL; C.I. No. 45350; Rolex Laboratories, India) were used as received. The structures of the dyes are presented in Fig. 2. The purity of the above compounds was c.a. 95–99%. Titanium tetra isopropoxide (Alfa Aesar) and glycine (S.D. Fine Chem., India) were used for the synthesis of CS TiO_2. Potassium dichromate ($K_2Cr_2O_7$), glacial acetic acid, ammonia solution and HPLC grade acetonitrile were obtained from Merck, India. Degussa P-25 TiO_2 was obtained from Degussa Corporation. Water was double distilled and filtered through Millipore (0.45 μm) filter before use.

2.2. Catalyst synthesis and characterization

Solution combustion technique was used to synthesize nano-sized anatase phase TiO_2. In this method, stoichiometric quantities of aqueous titanyl nitrate (prepared by the hydrolysis and subsequent nitration of titanium tetra isopropoxide) and glycine were combusted at 350 °C in a muffle furnace. A detailed synthesis methodology and the characterization of the catalyst are available

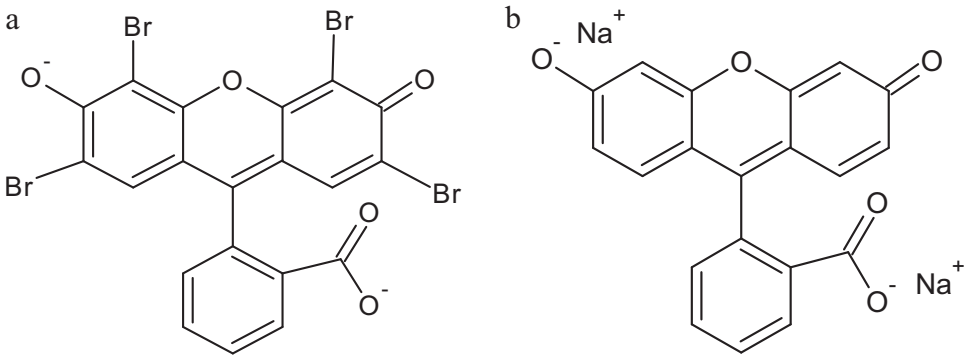

Fig. 2. Molecular structure of (a) eosin Y and (b) fluorescein (sodium salt).

Table 1
Characteristics of CS TiO_2 and P25.

Property	Technique used	CS TiO_2	P25
Particle size (nm)	TEM, XRD	8 ± 2 (anatase)	37 (anatase), 90 (rutile)
Band gap, eV	UV/vis	2.18, 2.65	3.1
Surface hydroxyl content (%)	TGA, FT-IR	15.5	1.3
BET surface area ($m^2\ g^{-1}$)	Porosimetry	150	50
pH_{zpc}	pH drift method	2.4	6.25

elsewhere [10,15,16]. Table 1 provides a summary of the characteristics of CS TiO_2 and the conventional P25 TiO_2. It is evident that TiO_2 synthesized by solution combustion technique is nano-sized, possesses a lower band-gap, higher surface area, higher surface hydroxyl content and a more acidic surface compared to P25.

2.3. Photoreactor

All the degradation experiments were carried out in a photocatalytic reactor. The reactor consisted of a jacketed pyrex reactor of 5.2 cm i.d. × 7.5 cm o.d. × 18.5 cm height, inside which a 400 W high pressure mercury vapor lamp was placed. The lamp radiated in the entire spectrum from 200 to 800 nm. However, the UV emission lines centered at 254, 313 and 365 nm were filtered using a liquid filter consisting of 0.5% aqueous $K_2Cr_2O_7$ solution. The thickness of the $K_2Cr_2O_7$ glass slit was 1 cm, which ensured that there was no leakage of the UV component of the incident radiation entering the reactor. The dye + phenolic compound + catalyst solution was taken in a cylindrical pyrex glass tube of 2.8 cm i.d. × 23.5 cm height. Oxygen was bubbled at a rate of 20 mL min^{-1}. The reactants were continuously stirred using a magnetic stirrer. Water circulation through the reactor jacket ensured that the temperature of the reaction mixture was maintained at 30 °C. The schematic of the experimental set up is provided in Fig. SI 1(a) (see supporting information). From Fig. SI 1(b) (see supporting information), it is clear that the peak emission wavelengths are centered at 410, 444, 555 and 590 nm. The intensity and photon flux of the light source determined by the photoisomerization of azobenzene [17] were 1.03×10^{-7} Einstein s^{-1} and 220 μW cm^{-2}, respectively.

2.4. Degradation experiments

Before irradiating the reactants, the mixture of dye + catalyst + phenolic solution was well stirred for 30 min in the dark in the presence of O_2, for the establishment of adsorption–desorption equilibrium. One hundred millilitre of the aqueous solution of dye and phenolic compound was exposed to visible light radiation in presence of 1 g L^{-1} of the catalyst and continuous bubbling of oxygen. All the reactions were carried out at the natural pH of the reaction mixture, in order to avoid the interfering effect of other cationic or anionic species. The degradation experiments were carried out for a total time period of 5 h, and aliquots of 1 mL were withdrawn at regular intervals to monitor the concentration of the dye and the phenol compound. All the samples were centrifuged to remove the catalyst prior to analysis.

2.5. Sample analysis

Different analysis techniques were adopted to characterize the degraded phenolic compound, dye, degradation intermediates, and the catalyst surface during the photocatalytic reaction. They are as follows: high pressure liquid chromatography (HPLC) to quantify the concentration of the phenolic compound, UV/visible spectroscopy to quantify the concentration of the dye in the solution and on the catalyst surface, total organic carbon (TOC) analysis to analyze the residual carbon content, mass spectrometry (MS) to identify the degradation products of the phenolic compounds and the dye, and photoluminescence (PL) spectroscopy to characterize the TiO_2 surface during reaction. Further details on the conditions employed in each of the above analytical techniques are outlined in SI 2 (see supporting information).

3. Mechanism of dye sensitized degradation

The proposed mechanism of dye sensitized degradation of phenolic compounds is partly based on the well understood mechanism of electron injection from the excited chromophore bound to the TiO_2 surface [1,18,19], and on the various experimental evidences in this work.

3.1. Adsorption

$$TiO_2 + D \underset{\lambda_{11'}}{\overset{\lambda_{1'1}}{\rightleftharpoons}} TiO_2 - D_{ads} \quad (1)$$

The first step in the sensitized degradation reaction is the adsorption of the dye on the surface of TiO_2. The pseudo first order rate coefficient ($\lambda_{1'1}$) for this adsorption step is proportional to the concentration of the dye [D]. The presence of both hydroxyl and carboxyl end groups in EY (Fig. 2) aids in the dissociative surface adsorption of this dye onto the surface hydroxyl ($Ti–OH_2^+$) sites of CS TiO_2 [20]. Fig. 3 shows the diffuse reflectance UV/vis absorption spectra of the aqueous EY solution, and EY adsorbed onto TiO_2 in

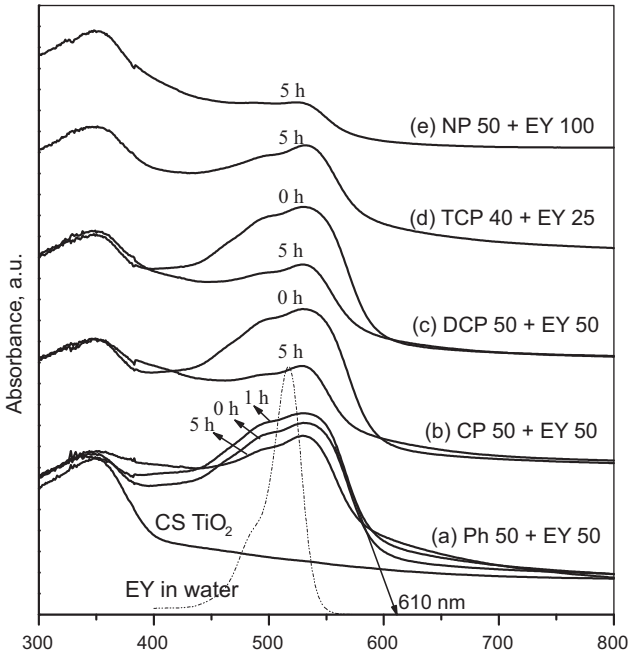

Fig. 3. Diffuse reflectance UV/vis spectra of EY adsorbed CS TiO_2 during the photocatalytic degradation of phenol, CP, DCP, TCP and NP. The unit of concentration of EY and the phenolic compound is in mg L^{-1}. Dotted line indicates the absorption spectra of EY in water.

the presence of the phenolic compounds. It is evident that EY is adsorbed on the acidic surface of CS TiO_2 (pH_{pzc} = 2.4), and shows a red shift in the absorption maximum from 517 nm to 530 nm, which is characteristic of the binding of EY to the surface hydroxyl groups of CS TiO_2 [21].

3.2. Excitation of the dye by visible light

$$TiO_2 - D_{ads} \underset{h\nu(\lambda>400\,nm)}{\overset{\lambda_{10}}{\longrightarrow}} TiO_2 - D^*_{ads} \quad (2)$$

This step signifies the absorption of the visible light photon ($\lambda > 400$ nm) by the adsorbed dye, and the formation of the excited state dye species (D^*). From the UV/vis spectra of EY adsorbed TiO_2, the absorption threshold for EY/CS TiO_2 was found to be 610 nm, which gives an estimate of the 0–0 transition energy (E_{0-0}) of 2.03 eV. The ground state redox potential for EY, corresponding to the highest occupied molecular orbital (HOMO) was reported to be 1.15 V (vs. NHE) [22]. Therefore, an estimate of the energy of the lowest unoccupied molecular orbital (LUMO) can be calculated as (LUMO = HOMO − E_{0-0}) − 0.88 V (vs. NHE) (Fig. 1). Thus, the dye is excited from HOMO to LUMO, where the fluorescence lifetime of EY is 1.4 nano seconds (ns) [20]. The rate of this reaction is proportional to the intensity of the incident visible radiation ([$h\nu$]).

3.3. Electron injection

$$TiO_2 - D^*_{ads} \overset{\lambda_{02}}{\longrightarrow} TiO_2(e^-) - D^{\bullet+}_{ads}\,(or)\,TiO_2(e^-) + D^{\bullet+}_{soln} \quad (3)$$

$$TiO_2 + e^-_{soln} + D^{\bullet+}_{soln} \overset{\lambda_{2'2}}{\longrightarrow} TiO_2(e^-) - D^{\bullet+}_{ads} \quad (4)$$

Photoexcitation of the dye is followed by the electron transfer reaction, which plays a vital role in the initiation of the reactions involving the degradation of the organic compounds. The driving force for this reaction is the potential difference between the LUMO of the excited dye and the conduction band edge of TiO_2 (E_{CB}), which is dependent on the pH of the solution, and given by $E_{CB} = -0.1 - 0.059 \times$ pH. Hence, the driving force for electron injection is calculated to be 0.6 V (vs. NHE) at a pH of 3. The time scale for the electron transport is dependent on the molecular structure of the sensitizer and the vibrational states of the semiconductor, and it is of the order of femto seconds (fs) [18]. Thus, electron injection proceeds at a much higher rate compared to the deactivation of EY to the ground state, which is of the order of ns. Moser and Grätzel [21] have evaluated by laser photolysis studies that the electron injection in EY/TiO_2 system proceeds at a rate of $8.5 \times 10^8\ s^{-1}$ at a pH of 3, with a quantum yield of 38%. The injected electron can, however, also delocalize from the TiO_2 surface to the bulk solution, or relax to the bottom of the conduction band to undergo recombination reaction.

The electron injection is accompanied by the concomitant formation of the dye radical cation ($D^{\bullet+}$) from the excited triplet state of EY. The possibility for the formation of the semireduced dye radical anion ($D^{\bullet-}$) is scarce due to the presence of TiO_2 as a heterogeneous medium. To validate the formation of the dye radical cation, we have recorded the PL spectrum of the 50 mg L^{-1} of EY loaded CS TiO_2 during the first hour of reaction with 50 mg L^{-1} of phenol. The PL spectrum in Fig. 4 shows that there is a small peak found at 460 nm corresponding to the formation of EY radical cation [21]. The other peaks signify the ground state and the triplet excited state of EY. We have also assumed that there is a possibility for $D^{\bullet+}$ to enter the bulk solution. This is validated by the fact that the dye undergoes decoloration during the degradation of phenol, which means that the degradation of $D^{\bullet+}$ can occur either on the surface of TiO_2 or in the bulk solution with the desolvated electrons and hydroxyl radicals.

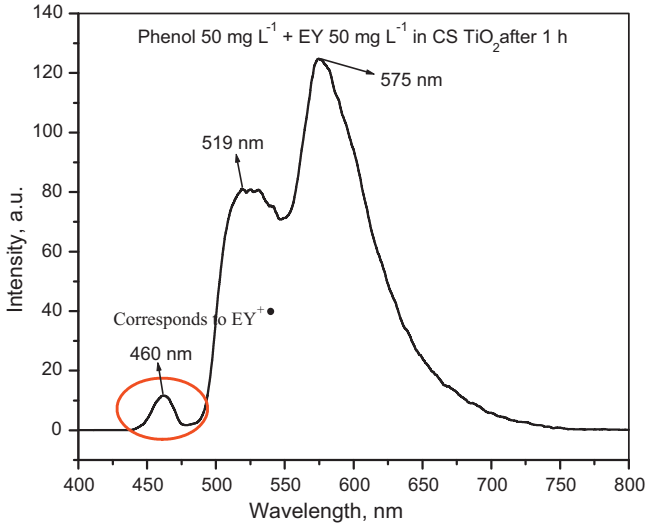

Fig. 4. Photoluminescence spectra of 50 mg L^{-1} EY loaded CS TiO_2 during the degradation of 50 mg L^{-1} of phenol. The excitation wavelength was at 440 nm.

Reaction (4) signifies the adsorption of the electron and the dye radical cation from the bulk solution onto the surface of TiO_2. Although this reaction proceeds at a slower rate compared to the electron injection and electron scavenging reactions, this is included for the sake of completeness of the detailed mechanism.

3.4. Recombination

$$TiO_2(e^-) - D^{\bullet+}_{ads} \overset{\lambda_{21}}{\longrightarrow} TiO_2 - D_{ads} \quad (5)$$

This reaction signifies the recombination of the dye radical cation with the injected electron to form the ground state dye [21]. Though this first order reaction step is 4000 times slower than the electron injection process, we have included this step in the mechanism of sensitized degradation for the sake of completeness.

3.5. Electron scavenging

$$TiO_2(e^-) - D^{\bullet+}_{ads} + O_2 \overset{\lambda_{23}}{\longrightarrow} TiO_2(O^{\bullet-}_2) - D^{\bullet+}_{ads} \quad (6)$$

This reaction represents the formation of superoxide radicals by the reaction of molecular oxygen with the trapped electron in the conduction band of TiO_2. This reaction also limits the recombination of the electrons with the dye radical cation to regenerate the dye. The pseudo first order rate coefficient for this reaction is dependent on the concentration of O_2 [O_2]. However, since O_2 was bubbled throughout the reaction at a constant flow rate with uniform stirring, the concentration is assumed to be saturated, and hence is treated as a constant.

3.6. Generation of hydroxyl species

$$TiO_2(O^{\bullet-}_2) - D^{\bullet+}_{ads} + H_2O \overset{\lambda_{34}}{\longrightarrow} TiO_2(OH^-) - D^{\bullet+}_{ads} + HO^{\bullet}_2 \quad (7)$$

$$TiO_2(OH^-) - D^{\bullet+}_{ads} \overset{\lambda_{45}}{\longrightarrow} TiO_2(OH^{\bullet}) - D_{ads} \quad (8)$$

$$TiO_2 - D^*_{ads} + H_2O \overset{\lambda_{06}}{\longrightarrow} TiO_2(OH^{\bullet}) - DH^{\bullet}_{ads} \quad (9)$$

$$TiO_2(OH^{\bullet}) - DH^{\bullet}_{ads} + O_2 \overset{\lambda_{65}}{\longrightarrow} TiO_2(OH^{\bullet}) - D_{ads} + H^+ + O^{\bullet-}_2 \quad (10)$$

$$TiO_2(OH^{\bullet}_{surface}) + D \overset{\lambda_{5'5}}{\longrightarrow} TiO_2(OH^{\bullet}) - D_{ads} \quad (11)$$

The above set of reactions indicates the different routes by which the hydroxyl radicals are generated with the simultaneous regeneration of the dye species. Reaction (7) represents the formation of the hydroxyl anion and hydroperoxy radicals from the aqueous medium by the interaction with the superoxide radicals. Reaction (8) denotes the formation of hydroxyl radicals with the simultaneous regeneration of the dye in the ground state. Reactions (9) and (10) show the pathway by which the hydroxyl radicals are generated directly from the excited state of the dye. Accordingly, the semireduced form of the dye ($DH^{\bullet}$), which is usually the semiquinone form, is formed in the ground state [19]. Owing to the high reactivity, these radicals are converted back to the original dye species by the reaction with O_2. Reaction (11) represents the adsorption of the dye onto the surface hydroxyl sites of the TiO_2.

3.7. Adsorption and degradation of the phenolic compound

$$TiO_2(OH^{\bullet}) - D_{ads} + Ph \underset{\lambda_{75}}{\overset{\lambda_{57}}{\rightleftharpoons}} TiO_2(OH^{\bullet}) - D_{ads} - Ph_{ads} \quad (12)$$

$$TiO_2(OH^{\bullet}) - D_{ads} - Ph_{ads} \xrightarrow{\lambda_{71}} TiO_2 - D_{ads} + ROF \rightarrow CO_2 + H_2O \quad (13)$$

The phenolic compounds degrade by initially getting adsorbed onto the surface of the dye adsorbed TiO_2. The pseudo first order rate coefficient for the adsorption step (λ_{57}) is proportional to the concentration of the phenolic compound. The attack of the hydroxyl radicals on the phenolic compounds results in the formation of hydroxylated intermediate species leading to the formation of carboxylic acids as ring opened fragments and finally resulting in the mineralization to CO_2 and H_2O.

3.8. Degradation of the adsorbed dye

$$TiO_2(OH^{\bullet}) - D_{ads} \xrightarrow{\lambda_{55'}} TiO_2 + \text{Degraded dye} \quad (14)$$

$$TiO_2 - D^{\bullet+}_{ads}\,(\text{or})\,TiO_2 + D^{\bullet+}_{soln} \xrightarrow{\lambda_{22'}} TiO_2 + \text{Degraded dye} \quad (15)$$

The degradation of the phenolic compounds is also accompanied by the degradation of the dye (Fig. 3). Reactions (14) and (15) represent the degradation of the ground state dye by the attack of hydroxyl radicals, and the dye radical cation by the interaction with superoxide radicals, respectively. These reactions compete with the degradation of phenolic compounds (reactions (12) and (13)). Previous studies have shown that $D^{\bullet+}$ is one of the important precursors for the degradation of the dye [1,23].

4. Model formulation

We have formulated the above reactions (1)–(15) in the form of a cyclic network to arrive at the rate equation for the degradation of the phenolic compound. Scheme 1 shows the pyramidal network mechanism, where the adsorbed dye (X_1), adsorbed dye radical cation (X_2) and the adsorbed hydroxyl species (X_5) form the node points of the base cycle. These three intermediate species interact directly with bare TiO_2 according to reactions (1), (4), (14) and (15). The central node connecting the different pathways is the excited state dye (X_0). Chen and Chern [11] have derived a framework for solving such networks and applied this methodology for the enzymatic dihydrofolate reaction. In the current work, we have also used the network reduction technique to derive the rate equation for the degradation of phenolic compounds. The applicability of network reduction for the heterogeneously catalyzed reaction in Scheme 1 is based on the fact that all the TiO_2 adsorbed intermediates are present at trace levels, i.e., pseudo steady state assumption can be used for all the radical species, and the rate coefficients signifying each and every step are first order in the concentration of the reactants.

The solution technique lies in transforming the internal Y branch of the network to a delta loop connecting X_1, X_2 and X_5. Once this transformation is achieved, the entire network can be treated as a single cycle with the loop coefficients replacing the delta loops. We have provided a detailed derivation of the rate equation in Appendix A. Figs. SI 3 and SI 4 (see supporting information) depict the Y-to-delta transformation and the reduced single cycle network of the reaction network in Scheme 1, respectively. The final rate expression is given by

$$r = -\frac{d[Ph]}{dt} = \frac{[Ph][D][TiO_2]}{K_1^{-1}[Ph][D] + K_2^{-1}[Ph] + K_3^{-1}[D] + K_4^{-1}} \quad (I)$$

where [Ph], [D] and [TiO_2] signify the concentration of the phenolic compound, dye and TiO_2, respectively. The lumped rate coefficients K_1, K_2, K_3 and K_4 are given by $K_1'K_4'/K_8'$, $K_1'K_4'/K_7''$, $K_1'K_4'/K_6'$ and $K_1'K_4'/K_6''$, respectively. The expressions for the above lumped rate coefficients are provided in Appendix A, Eqs. (A.25)–(A.28), (A.32)–(A.34) and (A.38)–(A.40). The expressions for the rate coefficients contain light intensity ([$h\nu$]) and oxygen concentration ([O_2]) as tunable quantities. However, in this study, we will be restricting our attention to the degradation of the phenolic compounds at a constant light intensity and a saturated oxygen concentration. The rate expression shows that the degradation of the phenolic compound depends on the concentration of the dye, phenolic compound and the interaction of the dye with the phenolic compound. We have adopted the initial rate method to evaluate the rate coefficients signifying the contribution of each of the components to the rate of degradation of the phenolic compound. Thus, by inverting Eq. (I) and rearranging, we arrive at the following expression

$$-\frac{1}{r_{0,Ph}} = \frac{1}{[TiO_2]}\left[\left(\frac{1}{K_1} + \frac{1}{K_2[D]_0}\right) + \frac{1}{[Ph]_0}\left(\frac{1}{K_3} + \frac{1}{K_4[D]_0}\right)\right] \quad (II)$$

where $r_{0,Ph}$, $[Ph]_0$ and $[D]_0$ denote the initial rate of degradation of the phenolic compound, initial concentration of the phenolic compound, and the dye, respectively. Hence, by conducting experiments with different initial concentrations of the phenolic compound at two different initial concentrations of the dye, the rate coefficients K_1, K_2, K_3 and K_4 can be evaluated from the intercept and slope of Eq. (II).

5. Results and discussion

Initial experiments performed with different anionic and cationic dyes as sensitizers for the degradation of 50 mg L^{-1} of phenol with CS TiO_2 indicated that the cationic dyes like rhodamine B (xanthene-fluorene class), methylene blue (quinone imine class) and acriflavine (acridine class) were not adsorbed onto the surface of CS TiO_2 even at very low concentrations of 5–10 mg L^{-1}. This shows that the highly positive surface charge of CS TiO_2 repels the cationic dyes. Hence, the degradation of phenol was also not observed with these dyes. However, with anionic dyes like orange G (azo class), alizarin cyanine green (anthraquinone class) and indigo carmine (indigo class), significant adsorption of the dyes was observed in the initial dark adsorption period. But with visible light irradiation, the dyes themselves underwent oxidation, while the degradation of the phenolic compound was less than 6% of the original concentration at the end of 5 h. This shows that the regeneration rate of the dye according to reactions (8), (10) and (11) is negligible with these classes of dyes. Fig. SI 5 (see supporting information) depicts the pH response of CS TiO_2 at different pH regimes in aqueous medium.

Hence, all the reactions were carried out with EY and FL as the sensitizing dyes. All the degradation reactions were carried out at the natural pH of the dye + phenolic compound + catalyst solutions. The solution pH in the case of CS TiO_2 catalyzed reactions was 3.5 ± 0.1, while that with P25 was 6.5 ± 0.2 during the course of

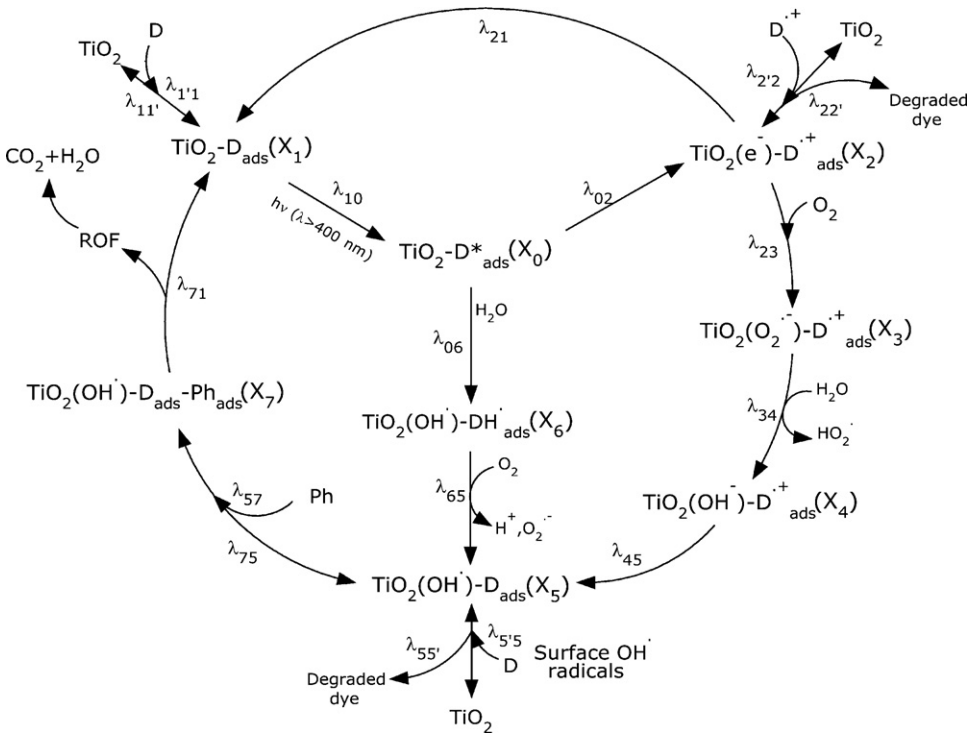

Scheme 1. Pyramidal network mechanism for the dye sensitized degradation of phenolic compounds.

degradation. This arises due to the very low pH_{zpc} of CS TiO_2 (2.4) compared to P25 (6.25). The initial adsorption of 50 mg L^{-1} of EY was 85% and less than 5% in the presence of 1 g L^{-1} of CS TiO_2 and P25, respectively. Therefore, for a fair comparison of the activity of P25 with CS TiO_2 for the initial adsorption of EY and the degradation of phenol, the pH of the P25 solution was adjusted to 3.5 ± 0.2 using dil. HNO_3. This showed a better adsorption of EY (60%) onto P25. Nevertheless, the percentage degradation of phenol at the end of 5 h did not improve significantly. While CS TiO_2 resulted in 66% of the degradation of phenol, the degradation was only 15% with P25 (Fig. 5). Similar results obtained for the degradation of other phenolic compounds employed in this study with P25 are discussed in Section 5.3.

The low activity exhibited by P25 can be attributed to the low surface area and surface hydroxyl content of P25 compared to CS TiO_2. Table 1 shows that the surface area of CS TiO_2 is 3 times that of P25 and the surface hydroxyl content is 10 times higher. Apart from these, P25 is composed of 37 nm and 90 nm anatase and rutile grains [24], respectively, in the ratio 20:80, while CS TiO_2 is 100% anatase with a particle size of 8 ± 2 nm. This means that the availability of a TiO_2 conduction band per electron injected from the excited state of the dye is higher in the case of CS TiO_2. Thus, higher surface area and surface hydroxyl content in CS TiO_2 results in an increase in the concentration of the dye and hydroxyl radicals adsorbed TiO_2 (species X_5) by reaction (11). Moreover, higher mean particle size of P25 can result in filtering of the incident visible light radiation from exciting the adsorbed dye species. This proves that CS TiO_2 acts as an efficient photocatalyst not only in the ultraviolet range, but also in the visible range.

5.1. Effect of initial dye concentration

Fig. 5 shows the degradation profiles of 50 mg L^{-1} of phenol at different conditions. The adsorption of phenol in the initial dark adsorption period is less than 6% for all the systems. It is clear that the absence of catalyst results in only 14% degradation of phenol, without any reduction in the dye concentration, over the entire time period of 5 h. Similarly, the absence of dye resulted in only 10% degradation of phenol in 5 h. This shows the importance of adsorbing EY onto TiO_2 for the photodegradation of phenol in the visible range, even though CS TiO_2 has an absorption band in the visible range. These control experiments suggest that the reaction is not just bimolecular in EY and phenol, and the presence of the catalyst and the adsorption of the dye are very important. To investigate the effect of initial concentration of EY on the degradation of phenol, multiple experiments were per-

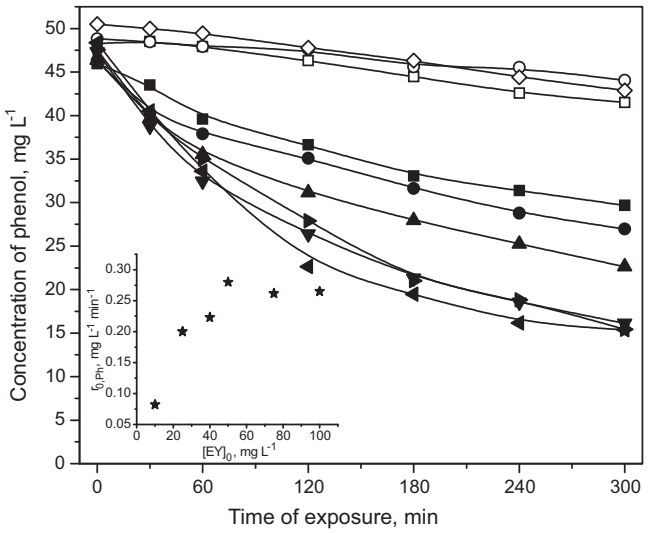

Fig. 5. Concentration profiles of 50 mg L^{-1} of phenol under different conditions. Inset: effect of initial concentration of EY on the initial rate of degradation of 50 mg L^{-1} of phenol. [Legend: (□) 50 mg L^{-1} EY without any catalyst, (○) 1 g L^{-1} CS TiO_2 without EY, (◊) 50 mg L^{-1} EY + 1 g L^{-1} P25 at pH – 3.7, (■) 10 mg L^{-1} EY, (●) 25 mg L^{-1} EY, (▲) 40 mg L^{-1} EY, (▼) 50 mg L^{-1} EY, (◄) 75 mg L^{-1} EY, (►) 100 mg L^{-1} EY, all solid symbols are with 1 g L^{-1} CS TiO_2].

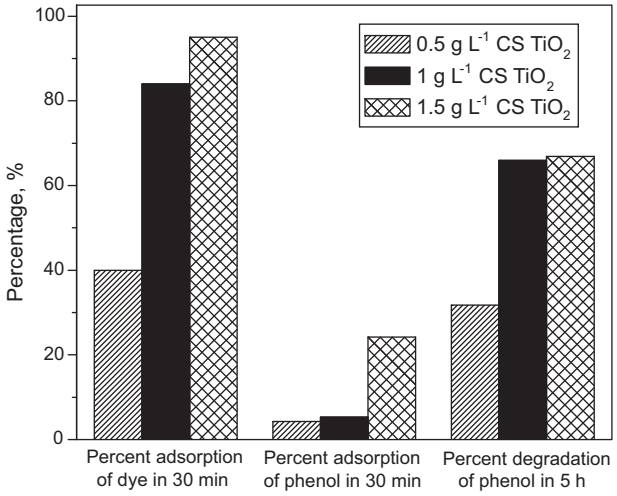

Fig. 6. Effect of loading of CS TiO_2 on the degradation of 50 mg L^{-1} of phenol with 50 mg L^{-1} of EY.

formed with 10–100 mg L^{-1} of EY for the degradation of 50 mg L^{-1} of phenol. The degradation rate increases with the initial concentration of EY till the EY concentration is 50 mg L^{-1}. Thereafter, the rate stabilizes and the final concentration of phenol was invariant with higher EY concentrations. The percent degradation of phenol at the end of 5 h with different initial concentrations of EY follows the order: 75 mg L^{-1} (68%) ≈ 100 mg L^{-1} (67.5%) ≈ 50 mg L^{-1} (66%) > 40 mg L^{-1} (51%) > 25 mg L^{-1} (41%) > 10 mg L^{-1} (35%). The inset in Fig. 5 depicts the variation of the initial rate of degradation of phenol with the EY concentration. It is hence clear that higher concentration of EY results in an increase in the concentration of EY in the liquid phase, thereby leading to the competition between the adsorption of phenol and EY on the surface of CS TiO_2. As the binding of EY onto TiO_2 is more probable due to the presence of carboxyl moiety, the adsorption of phenolic compounds is hindered. However, the presence of EY results in the sensitization and the hence the oxidation of phenol. This balance between the competitive adsorption and sensitization results in the rate of degradation of phenol to be unaffected by EY concentration. Therefore, further experiments with phenol and chlorophenols were carried out with 50 mg L^{-1} of EY and FL.

5.2. Effect of catalyst loading

In order to investigate the effect of loading of the catalyst, the degradation of 50 mg L^{-1} of phenol was carried out with 0.5, 1 and 1.5 g L^{-1} of CS TiO_2. Fig. 6 shows that the initial adsorption of the dye is enhanced in the presence of higher concentrations of the catalyst. However, increasing the loading higher than 1 g L^{-1} does not significantly enhance the degradation of phenol, as both 1 and 1.5 g L^{-1} loading of CS TiO_2 result in 66% degradation of phenol. Moreover, 1.5 g L^{-1} of CS TiO_2 also results in the higher initial adsorption of phenol. This is due to the increase in available TiO_2 surface centers, which results in the adsorption of phenol, even after the complete adsorption of EY. This indicates that there is also a possibility for the adsorption of the degradation intermediates, when the catalyst loading is higher. Therefore, an optimum concentration of the catalyst in dye sensitized systems is that amount which is just sufficient to adsorb the dye, as the excess amount of catalyst is inactive without the presence of the dye. Hence, we have used an optimum catalyst loading of 1 g L^{-1} for further experiments.

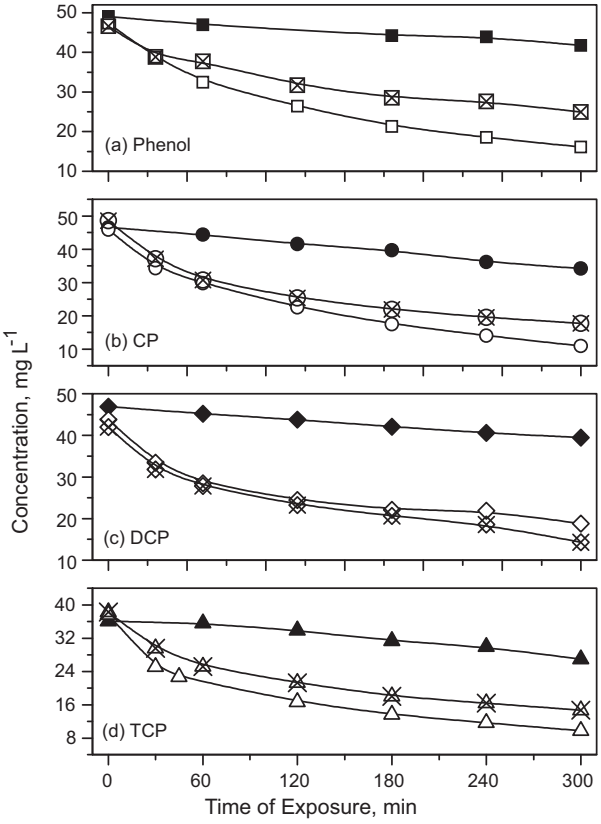

Fig. 7. Concentration profiles for the degradation of (a) phenol, (b) CP, (c) DCP and (d) TCP under different conditions. [Legend: open symbols – with EY and CS TiO_2, closed symbols – with EY and P25 at pH 3.5, crossed symbols – with FL and CS TiO_2].

5.3. Degradation of chlorophenols

Having optimized the concentration of the dye and the catalyst, we have carried out the degradation of CP, DCP and TCP with EY/CS TiO_2, FL/CS TiO_2 and EY/P25 (pH – 3.5) as the sensitizing systems. The diffuse reflectance UV/vis spectra in Fig. 3 shows that phenols and chlorophenols are adsorbed onto the surface of CS TiO_2 in the initial dark adsorption period, and at the end of the reaction, their concentration decreases, signifying the degradation of the dye on the surface of the catalyst. Alternatively, the intermediate products of degradation, which are usually the hydroxy substituted phenols adsorb on the surface of TiO_2, thereby displacing the dye or dye radical cation from the TiO_2 surface. The percent degradation of CP, DCP and TCP at the end of 5 h with EY/CS TiO_2 system was 76%, 58% and 74%, respectively (Fig. 7(b)–(d)). Fig. SI 6(a) (see supporting information) depicts the UV/vis spectra of EY adsorbed onto P25 at the end of 5 h during the degradation of CP and DCP, when the pH of the solution was adjusted to 3.5. It is clear that reducing the pH results in significant adsorption of EY onto P25. However, the degradation of CP, DCP and TCP were only 26%, 16% and 25%, respectively. This proves that the synergistic effect of surface area, surface hydroxyl content and particle size results in the higher activity of CS TiO_2 compared to P25.

FL belongs to the same dye class as EY and its molecular structure is similar to EY, without any bromine atoms. The molecular structure of FL is given in Fig. 2(b). Fig. SI 6(b) (see supporting information) shows the UV/vis spectra of FL adsorbed onto CS TiO_2 during the degradation of CP, DCP and TCP at the end of 5 h. It is clear that FL exhibits a good adsorption onto the surface of CS TiO_2 with an absorption threshold of 600 nm, which corresponds to a band gap energy of 2.07 eV, slightly higher than EY. The UV/vis spectra of aqueous FL after the initial adsorption period also indicated that

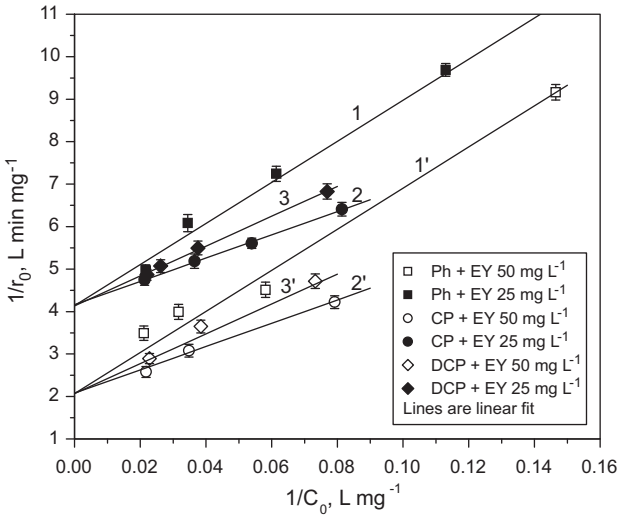

Fig. 8. Variation of inverse of initial concentration versus the inverse of initial rate for the degradation of phenol, CP and DCP with 25 and 50 mg L^{-1} EY.

the initial adsorption was 90–95% onto CS TiO_2 in presence of all the phenolic compounds used in this study. This is quite expected as both EY and FL adsorb onto TiO_2 through the carboxyl moiety present in their structure. From Fig. 7(a)–(d), it is evident that the degradation of phenol, CP and TCP sensitized by FL in the presence of CS TiO_2 was 30%, 17% and 17% lesser compared to that with EY as the sensitizer, respectively. For the degradation of DCP, both EY and FL exhibited similar degradation profiles initially, while at the end of 5 h, FL exhibited 10% higher degradation compared to EY. However, compared to the EY/P25 system, FL/CS TiO_2 exhibits 67%, 59%, 75% and 59% higher degradation of phenol, CP, DCP and TCP, respectively. These collectively indicate that apart from the adsorption of the dye onto the catalyst and the sensitizing mechanism, the degradation of the phenolic compound is also dependent on the interaction of the dye and the phenolic compound. Hence the structure of the dye assumes a vital role in such sensitizing reactions. From the mass spectrometric evidences in the current work (Section 5.5), it can be concluded that the presence of bromine in EY results in the hydroxylation of the dye at the position of bromine, thereby changing the pathway of degradation of the dye, and hence the rate of degradation of the phenolic compound. An alternative explanation for the high activity exhibited by EY/TiO_2 compared to FL/TiO_2 can be due to the faster electron injection kinetics in EY compared to FL.

5.4. Kinetic analysis

In order to evaluate the kinetics of degradation of the above phenolic compounds, and to show the applicability of the mechanistic rate equation we have derived in Section 4, we have conducted multiple experiments of the degradation of phenol, CP, DCP and TCP with EY as the sensitizer and CS TiO_2 as the catalyst. To evaluate the slope and intercept of Eq. (II), we have conducted the degradation of phenol, CP and DCP of four different initial concentrations with 50 mg L^{-1} and 25 mg L^{-1} of EY. Figs. SI 7–9 (see supporting information) show the concentration profiles of phenol, CP and DCP of different initial concentrations during degradation. Initial rates for different initial concentrations of the phenolic compounds were calculated for the first 15 min or 30 min of degradation. The error in the initial rates was less than 4%.

Fig. 8 shows the plot of inverse of initial concentration versus the inverse of initial rate, according to Eq. (II), for the degradation of phenol, CP and DCP in presence of two different initial concentrations of EY. The lines are linear fit of the experimental data with an R^2 value of 0.98–0.99. It is evident that, for any particular phenolic compound, the slopes of the linear line joining the points (eg., lines 1 and 1′; 2 and 2′; 3 and 3′) are the same for both 25 mg L^{-1} and 50 mg L^{-1} of EY. This shows that the slope of the equation given by $(K_3^{-1} + K_4^{-1}[D]_0^{-1})$ is the same irrespective of the initial concentration of the dye ($[D]_0$). This means that the rate coefficient K_4 is zero. Similarly, the intercepts for phenol, CP and DCP with 25 mg L^{-1} and 50 mg L^{-1} of EY were 4.138 ± 0.01 L min mg^{-1} and 2.07 ± 0.01 L min mg^{-1}, respectively. Thus, by solving the equation signifying the intercept, given by $(K_1^{-1} + K_2^{-1}[D]_0^{-1})$, using the above values for the two initial concentrations of EY, it was found that the rate constant K_1 is zero and K_2 is equal to $9.67 \pm 0.35 \times 10^{-3}$ L mg^{-1} min^{-1}. Hence, the rate equation effectively reduces to the form given by

$$-\frac{1}{r_{0,\mathrm{Ph}}} = \frac{1}{[\mathrm{TiO_2}]}\left(\frac{1}{K_2[\mathrm{D}]_0} + \frac{1}{K_3[\mathrm{Ph}]_0}\right) \quad \text{(III)}$$

In order to get a physical understanding of the rate coefficients K_2 and K_3, given by $K_1'K_4'/K_7''$ and $K_1'K_4'/K_6'$, we have expanded them based on the lumped terms given by Eqs. (A.25), (A.28), (A.34) and (A.39) (see Appendix A). Thus, K_2 and K_3 are given by

$$K_2 = \kappa \frac{k_{1'1}}{k_{11}} k_{10}[h\nu] \quad \text{(IV)}$$

$$K_3 = \kappa \frac{k_{57}k_{71}}{k_{75} + k_{71}} \quad \text{(V)}$$

$$\kappa = \left[1 + \frac{k_{2'2}}{k_{22'}} + k_{23}[\mathrm{O_2}]\frac{k_{2'2}}{k_{22'}}\left(\frac{1}{k_{34}} + \frac{1}{k_{45}}\right)\right]\frac{k_{02}}{(k_{02} + k_{06})} \quad \text{(VI)}$$

Therefore, it is clear that both the rate coefficients share a common term κ, which includes the individual rate coefficients signifying (i) the injection of electron and the formation of the dye radical cation (k_{02}), (ii) oxidation of the dye radical cation ($k_{2'2}$ and $k_{22'}$), (iii) formation of the hydroxyl species by superoxide radicals (k_{34} and k_{45}) and (iv) the formation of hydroxyl species from aqueous phase (k_{06}). Apart from these, K_2 depends on the adsorption–desorption ($k_{1'1}$ and $k_{11'}$) and the excitation of the dye (k_{10}), while K_3 depends on the adsorption–desorption (k_{57} and k_{75}) and the degradation of the phenolic compound (k_{71}). It is thus clear that K_2 signifies the contribution of the adsorbed dye to the sensitization process, while K_3 signifies the degradation of the phenolic compound. Henceforth, it is appropriate to denote K_2 and K_3 as K_D and K_Ph, respectively. Inverting Eq. (III) we get the final rate equation as

$$r_{\mathrm{Ph}} = -\frac{\mathrm{d[Ph]}}{\mathrm{d}t} = \frac{K_\mathrm{D}K_\mathrm{Ph}[\mathrm{Ph}][\mathrm{D}][\mathrm{TiO_2}]}{K_\mathrm{D}[\mathrm{D}] + K_\mathrm{Ph}[\mathrm{Ph}]} \quad \text{(VII)}$$

A careful investigation of Eq. (IV) shows that K_D is dependent on the intensity of the incident radiation, $[h\nu]$. Although all the reactions have been carried out at a constant intensity of the light source, the degradation of the dye, which is the principle absorber of radiation, might affect the intensity of the incident radiation reaching the catalyst surface. This might reduce the degradation rate of the phenolic compound. However, according to the present experimental condition, the total moles of incident photons correspond to 370 μM s^{-1}, which is lower. Hence, we have considered that the rate coefficient K_D is unaffected by the small changes in the intensity caused by the degradation of the dye on the catalyst surface.

As all the experiments were carried out at a constant loading of CS TiO_2, the rate is independent of $[TiO_2]$. Thus four rate coefficients appearing in Eq. (II) have been successfully reduced to two based on the above kinetic analysis. A closer investigation of Eq. (VII) indicates that, when $[D] \gg [Ph]$, the contribution of $K_{Ph}[Ph]$

Table 2
Rate coefficients for EY sensitized degradation of phenol, CP, DCP and TCP per mg L^{-1} of CS TiO_2.

Phenolic compound	K_D ($\times 10^{-3}$ L mg^{-1} min^{-1})	K_{Ph} ($\times 10^{-2}$ L mg^{-1} min^{-1})
Phenol	9.67 ± 0.35	2.07 ± 0.10
4-Chlorophenol	9.67 ± 0.35	3.65 ± 0.17
2,4-Dichlorophenol	9.67 ± 0.35	2.84 ± 0.10
2,4,6-Trichlorophenol	10.14 ± 0.30	3.06 ± 0.12

in the denominator is negligible and hence, the rate of degradation of the phenolic compound is first order in [Ph], with K_{Ph} as the first order rate coefficient. Similarly, when [Ph] ≫ [D], K_D[D] in the denominator is negligible, the rate of degradation of the phenolic compound is first order in [D], with K_D as the degradation rate coefficient. This means that, at high concentrations of the dye, the rate is independent of [D] and depends only on [Ph], whereas at high concentrations of the phenolic compound, the rate is independent of [Ph] and depends only on [D]. In order to verify this, we have conducted the degradation of TCP under the above two extreme cases. It is to be noted that high concentrations of the dyes and phenolic compounds correspond to 50–200 mg L^{-1}, which are a commonplace in effluent streams.

Fig. 9 shows the first order plots for the degradation of TCP, when (i) TCP concentration is between 2 and 20 mg L^{-1} in the presence of 100 mg L^{-1} of EY, and (ii) TCP concentration is 88 ± 3 mg L^{-1} in the presence of 2–8 mg L^{-1} of EY. The linear fit of the equation with R^2 of 0.99 shows that the limiting conditions are indeed valid, provided that the concentration of the dye or the phenolic compound is high enough, so that one of the terms in the denominator of Eq. (VII) can be safely ignored.

Importantly, we have observed that the rate coefficient K_D determined for the degradation of TCP, which is $10.14 \pm 0.30 \times 10^{-3}$ L mg^{-1} min^{-1}, is in close agreement with that determined for phenol, CP and DCP (Table 2). This shows that this rate coefficient is independent of the phenolic compound, and dependent only on the sensitizing dye. This means that the sensitization process, involving the injection of electron, the formation of dye radical cation, and the abstraction of the injected electron by O_2 to form superoxide and hydroxyl species, is unaffected by the presence of the phenolic compound, which is also validated by Eq. (IV). Based on the rate coefficient K_{ph}, which we have determined for the different phenolic compounds, it can be concluded that K_{Ph} follows the order: CP > TCP > DCP > phenol. From Table 2, it is clear that K_{Ph} for CP is 16%, 22% and 43% higher compared to that for TCP, DCP and phenol, respectively. The slowest degradation of phenol can also be ascertained from the UV/vis spectra in Fig. 3. The lesser reduction in absorbance of the EY peak even after 5 h for the degradation of phenol compared to other phenolic compounds elucidates that the degradation of the dye is not significant, as phenol has not degraded appreciably. The order of degradation of the phenolic compounds we have observed in this study using visible light source, is in contrast with that previously reported for the degradation in the presence of UV irradiation [25]. Generally, multiple substituted chlorophenols exhibit higher degradation rates compared to mono substituted chlorophenols and phenol. Although the degradation rate coefficient of phenol is lower compared to that of chlorophenols, DCP and TCP show lower degradation compared to CP. The lower rate of degradation observed for DCP and TCP can be due to the steric or electronic interaction between the chloride species from DCP and TCP, and the bromide species attached to EY (Section 5.5). This is probable, as the phenolic compounds and the dye are in close contact on the surface of TiO_2. Thus the change in orbital conformation and electrostatic interactions might lead to a lesser reactivity of DCP and TCP compared to CP.

5.5. Mechanism of degradation of the phenolic compounds and EY

It is well accepted that hydroxylation is the most important step that results in the degradation of the phenolic compounds during photocatalysis. Hydroxyl radicals are usually considered to be the major species responsible for photocatalysis based on the evidence that includes the detection of hydroxylated intermediates, distribution of the hydroxylation products, and spin trapping with subsequent ESR detection [9,23]. The replacement of a proton by a hydroxyl group proceeds by two steps: the first one involves the substitution of hydroxyl groups in the ortho- and para-positions in the phenolic compound, followed by the ring opening of the hydroxylated compound to form aliphatic carboxylic acids. At sufficiently long exposure periods, these organic acids mineralize to form CO_2 and H_2O.

In the current work, we have used LC–MS for the identification of the different intermediates that are formed during the degradation of the phenolic compounds and the dye, EY. Thus, the samples collected at different time periods were analyzed for the intermediates and the degradation pathways for phenol, CP, DCP and TCP are suggested. Scheme 2 depicts the suggested pathway of degradation along with the molecular weight of the identified intermediates. As the ionization techniques employed in the mass spectrometer were ES or APCI, the molecular ion and the isotope peaks were only observed in the chromatogram. An important observation is that, mono-hydroxylated phenolic compounds like catechol and hydroquinone (molecular weight (MW) = 110) were not observed in the degraded samples during the sensitized degradation of phenol and CP. Hydroquinone was also not observed in the LC and MS as benzoquinone. However, pyrogallol (PY; MW = 126) and hydroxy hydroquinone (HHQ; MW = 126), which are di-hydroxylated species, were observed at low concentrations (less than 6 mg L^{-1}) during the initial periods of degradation. Although the formation of catechol and hydroquinone are a prerequisite for the formation of PY and HHQ, the near absence of these intermediates suggests that the consumption of these intermediates for the next hydroxylation step is faster compared to its formation. At long time periods, cleavage of the benzene ring of PY and HHQ between the hydroxyl species takes place, which results in the formation of hydroxy muconic acid (MW = 158) and muconic acid (MW = 142). Górska et al. [26] have also observed this intermediate during the visible light degradation of phenol with N- and C-doped TiO_2.

Li et al. [27,28] have investigated the mechanism of photocatalytic degradation of CP and some hydroxy chlorophenols by following the fragmentation of the intermediates of degradation. They have proposed the chlorocatechol and hydroquinone pathways for the formation of the intermediates during the degradation of CP. Many of the hydroxylated and ring opened intermediates, which we have observed during the sensitized degradation of CP, DCP and TCP agree well with those reported by Li et al. The first step in the degradation of CP is the formation of 4-chlorocatechol (MW = 144) and hydroquinone. 4-Chlorocatechol undergoes hydroxylation at ortho-position to chlorine, which later undergoes ring fragmentation between 1 and 2 positions to give 2,4-dihydroxy 3-chloro muconic acid (MW = 208). In a parallel reaction, HHQ is formed from hydroquinone and 4-chlorocatechol. Cheng et al. [29] have observed HHQ formation during the degradation of CP under visible light in the presence of CS TiO_2. The final step involves the formation of hydroxy muconic acid. Similarly, DCP initially forms 4-chlorocatechol and 2-chlorohydroquinone (MW = 144), followed by the hydroxylation and ring cleavage to form chloro-substituted hydroxyl muconic acids (MW = 208). It was observed that these species exist in the form of dianion due to adsorption onto the acidic TiO_2 surface.

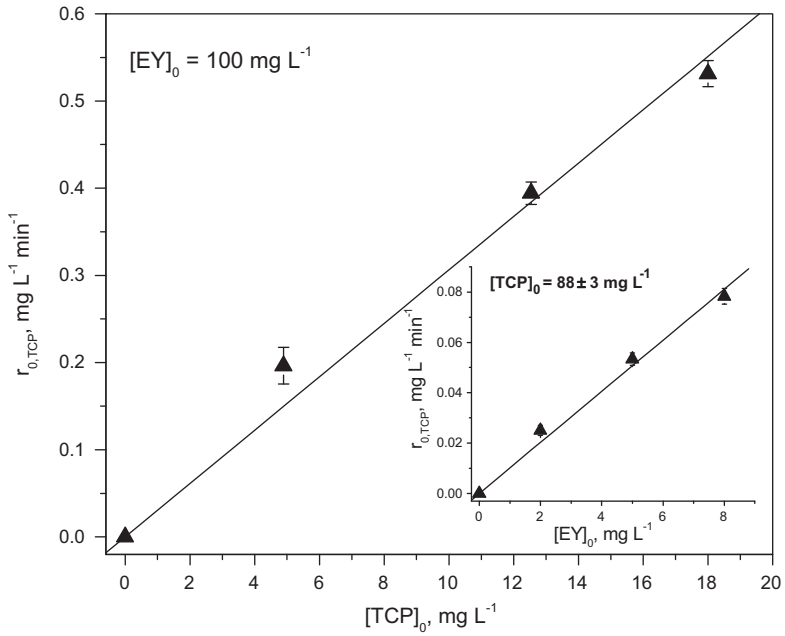

Fig. 9. First order rate curve for the degradation of TCP in presence of 100 mg L^{-1} of EY. Inset: Variation of the rate of degradation of 88 mg L^{-1} of TCP with the initial EY concentration.

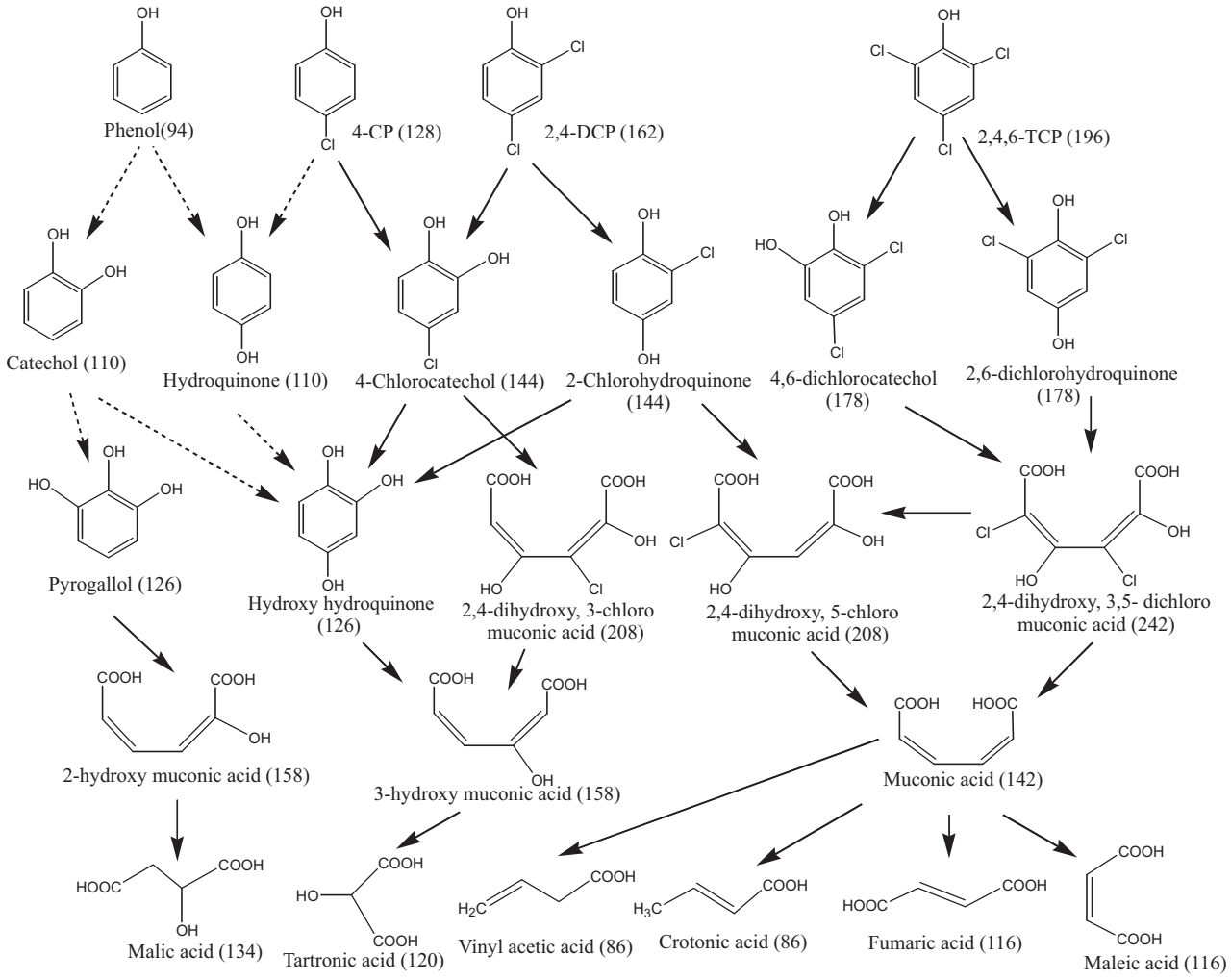

Scheme 2. Mechanism of formation of phenolic intermediates and ring opened fragments during the sensitized degradation of phenol, CP, DCP and TCP, identified by LC–MS. The molecular weights of the intermediates are given in braces.

The degradation of TCP involves the formation of dichlorocatechol and dichlorohydroquinone (MW = 178) in the initial step, followed by the hydroxylation and ring cleavage to form dihydroxy dichloro muconic acids (MW = 242). These acids were also observed to exist in the deprotonated form due to the association with the TiO_2 surface. Once muconic acid or its hydroxyl analogues are formed, the final step involves the formation of low MW organic acids like tartronic acid (MW = 120), fumaric acid (MW = 116), maleic acid (MW = 116), malic acid (MW = 134), vinyl acetic acid (MW = 86) and crotonic acid (MW = 86). At long exposure periods, these acids mineralize to CO_2 and H_2O.

In addition to the degradation of the phenolic compounds, the degradation of the dye was also observed during the course of reaction. Hence, the dye intermediates were also observed in the mass spectrum of the reaction samples. We have observed that the abstraction of bromine from EY occurs, which results in the formation of HBr (MW = 80). Our observation is also supported by the results of Zhang et al. [30], who have also monitored the time evolution of bromide ions (Br^-) during the degradation of EY in aqueous TiO_2 dispersions. Thus, the debromination sites in the EY molecule act as centers for hydroxylation by the attack of the hydroxyl radicals. This results in the bond rupture resulting in the opening of the EY ring structure. Along with HBr, other brominated intermediates, with 1–4 Br atoms in the structure were identified based on the relative abundance of the MW + 2, MW + 4 and MW + 6 peaks corresponding to Br. The actual MW of the intermediates, which correspond to the hydroxylated and ring opened intermediates of EY were found to be 294, 302, 332, 373 and 458 g mol^{-1}. Moreover, a low MW fragment of 148 g mol^{-1} containing only C, H and O was observed during the degradation of all the phenolic compounds. The accurate structure of these intermediates could not be established, as this would involve studying the fragmentation pattern of these intermediates in an electron impact ionization or MS/MS system. However, this analysis shows that the dye sensitized degradation involves a complex interaction of the dye, phenolic compound and the intermediates that originate from both the dye and the phenolic compound.

5.6. Mineralization of the phenolic compound + dye solution

In order to assess the mineralization of the dye sensitized systems and the stability of the intermediates, TOC analysis of the dye + phenolic compound was performed during the course of reaction. Fig. SI 10 (see supporting information) shows the time evolution of the TOC concentration during the degradation of the phenolic compounds sensitized by EY and FL in the presence of CS TiO_2. It is clear that in the initial time period of 1 h, nearly 20–30% mineralization was observed. This can be attributed to the adsorption of the unadsorbed dye in solution, as the adsorbed dye on the catalyst surface degrades during the course of reaction. Thereafter, the mineralization rate was slower and almost all the systems sensitized by EY exhibited a total mineralization of 35–42%. For the degradation of 15 mg L^{-1} of CP, nearly 45% and 55% reduction of TOC was observed in the initial time period of 1 h and final time period of 5 h, respectively, which is due to the low initial concentration of CP. However for the FL sensitized degradation of CP, both the initial reduction of TOC and the final TOC were less than that sensitized by EY, which clearly reflects the trends in the degradation of CP, when sensitized by EY and FL (Fig. 7(b)). Hence, the mineralization in dye sensitized systems is a complex quantity, which is governed by the desorption of the dye from the catalyst surface, degradation of the dye and the phenolic compound. From our experiments, it is clear that still longer exposure hours are required to achieve complete mineralization.

Finally, in order to evaluate the degradation of nitrophenolic compounds with the dye sensitized system, 50 mg L^{-1} of NP was degraded in the presence of EY and CS TiO_2. It was observed that, in the initial time period of 1 h, 15% of degradation of NP was observed, and thereafter the concentration remained the same, without any appreciable reduction. This was accompanied by the rapid degradation of the adsorbed EY. Fig. 3(e) shows the UV/vis spectra of 100 mg L^{-1} of EY adsorbed CS TiO_2 during the degradation of NP at 5 h. It is evident that the adsorption of EY is very less onto CS TiO_2 compared to that with the other phenolic compounds. Dieckmann and Gray [31] have previously observed that the degradation of NP is accompanied by the formation of inorganic nitrogen species like nitrite, nitrate and ammonium ions. These inorganic intermediates might result in the desorption of the dye from the surface of TiO_2, which result in the degradation of the dye radical cation in the aqueous solution, according to reaction (15). Hence our future work will address the development of efficient sensitizing systems for the degradation of such compounds, where the formation of anionic intermediates causes deleterious effect on the overall degradation of the organic contaminants.

6. Conclusions

In the current work, we have successfully demonstrated the dye sensitized degradation of phenolic compounds in presence of visible light radiation using nano-TiO_2 as the catalyst. TiO_2 synthesized by solution combustion methodology exhibited superior activity compared to the conventional P25 TiO_2 photocatalyst for the degradation of phenol, CP, DCP and TCP in the presence of EY as the sensitizing dye. During the reaction, it was found by UV/vis spectroscopy that the degradation of the phenolic compound is also accompanied by the degradation of the dye and desorption of the dye intermediates from the surface of TiO_2. Based on the experimental evidences, the mechanism of sensitized degradation was proposed, which includes the adsorption and desorption of the dye, excitation of the dye, electron injection to the conduction band of TiO_2, formation of the semi-oxidized dye radical cation, recombination of the electron and dye radical cation, generation of hydroxyl species, regeneration of the dye, adsorption, degradation and desorption of the phenolic compound, and the degradation of the dye. The formation of the dye radical cation species was confirmed by photoluminescence measurements. The mechanism was formulated in the form of a pyramidal network and the kinetic model for the rate of degradation of the phenolic compound was derived using the network reduction technique. An important outcome of the kinetic analysis employed in this work shows that the degradation rate of the phenolic compound is first order with respect to the concentration of the phenolic compound at sufficiently high concentrations of the dye, while the degradation rate is first order with respect to the high concentration of the dye at sufficiently high concentrations of the phenolic compound. The rate coefficient signifying the contribution of the dye (K_D) was found to be invariant for the different phenolic compounds, signifying that the sensitization process, which involves the excitation of the dye and electron injection is independent of the presence of the phenolic compound. The rate coefficient signifying the degradation of the phenolic compound (K_{Ph}) followed the order: CP > TCP > DCP > phenol. The intermediates that were formed during the degradation of the phenolic compounds were traced by mass spectroscopy and a plausible pathway of degradation of the phenolic compounds was established. All the phenolic compounds resulted in the formation of muconic acid and its hydroxy derivatives, before mineralization to CO_2 and H_2O. In totality, the encouraging results of this work shows that dye sensitized systems are potential candidates for the effective mineralization of organic contaminants under solar/visible radiation. Furthermore, such systems are classic models of “real” waste water, which are composed of more than one component, where the degradation of one component is affected by the other.

Acknowledgements

The authors thank Dr. K.R. Prasad of Organic Chemistry, Indian Institute of Science for useful discussions in the interpretation of mass spectra. The corresponding author thanks the Department of Science and Technology, India for the financial support and Swarnajayanthi Fellowship.

Appendix A. Derivation of rate equation by network reduction

The pyramidal network with side branches at X_1, X_2 and X_5, as shown in Scheme 1, can be reduced to a single cyclic network by the application of *Y*-to-delta transformation, derived earlier by Chen and Chern [11]. According to this transformation, the branches, X_1–X_0, X_0–X_2 and X_0–X_6–X_5 that constitute the central Y are transformed into closed loops comprising the following pathways, viz., X_1–X_0–X_2–X_1, X_0–X_2–X_3–X_4–X_5 and X_0–X_6–X_5, and X_1–X_0–X_6–X_5–X_7–X_1. These loops are replaced by the loop coefficients, L_{12} and L_{21}, L_{25}, and L_{51} and L_{15}, respectively. Fig. SI 3 (see supporting information) shows the branches that are accounted in the Y-to-delta transformation, and Fig. SI 4 (see supporting information) depicts the reduced cyclic network after combining the interior branches into a single loop coefficients.

For arbitrary nodes X_i, X_j and X_k in the base cycle, which are connected by a central node X_0, the lumped coefficients for the delta type network are given by [11]

$$\Gamma_{ik} = \frac{\Lambda_{i0}\Lambda_{0k}}{\Lambda_{0i} + \Lambda_{0j} + \Lambda_{0k}} \tag{A.1}$$

and so on for Γ_{ki}, Γ_{ij}, Γ_{ji}, Γ_{jk} and Γ_{kj}.

The loop coefficients for the single cycle network are given by

$$L_{ik} = \Lambda_{ik} + \Gamma_{ik} \tag{A.2}$$

and so on for L_{ki}, L_{ij}, L_{ji}, L_{jk} and L_{kj}. The Λ terms denote the branch coefficients given by

$$\Lambda_{jk} = \frac{\sum_{i=j}^{k-1} \lambda_{i,i+1}}{D_{jk}} \tag{A.3}$$

where

$$D_{jk} = \sum_{i=j+1}^{k} \left(\prod_{m=j+1}^{i-1} \lambda_{m,m-1} \prod_{m=i}^{k-1} \lambda_{m,m+1} \right) \tag{A.4}$$

Hence for the mechanism in Scheme 1, the loop coefficients are given by

$$L_{12} = \frac{\lambda_{10}\lambda_{02}}{\lambda_{02} + \Lambda_{05}} = \frac{\lambda_{10}\lambda_{02}}{\lambda_{02} + \lambda_{06}} \tag{A.5}$$

$$L_{15} = \frac{\lambda_{10}\Lambda_{05}}{\lambda_{02} + \Lambda_{05}} = \frac{\lambda_{10}\lambda_{05}}{\lambda_{02} + \lambda_{05}} \tag{A.6}$$

$$L_{21} = \lambda_{21} \tag{A.7}$$

$$L_{25} = \Lambda_{25} = \lambda_{23} \tag{A.8}$$

$$L_{52} = 0 \tag{A.9}$$

$$L_{51} = \Lambda_{51} = \frac{\lambda_{57}\lambda_{71}}{\lambda_{75} + \lambda_{71}} \tag{A.10}$$

The rate of degradation of the phenolic compound or the steady state rate through the cycle is given by [11]

$$r = -\frac{\mathrm{d[Ph]}}{\mathrm{d}t} = \frac{\Delta}{D}[X_T] \tag{A.11}$$

where

$$\Delta = \prod_{l=0}^{n} L_{l,l+1} - \prod_{l=0}^{n} L_{l+1,l} \tag{A.12}$$

D refers to the total sum of the *D* coefficients defined by Eq. (A.4) for all the species in the base cycle and in the internal *Y* branches given by Chen and Chern [11].

$[X_T]$ is the total concentration of the catalyst inclusive of all the intermediate states given by

$$[X_T] = [\mathrm{TiO_2}] + \sum_{i=0}^{7} [X_i] \tag{A.13}$$

$$[X_i] = f([\mathrm{TiO_2}], [h\nu], [\mathrm{O_2}], [\mathrm{D}], [\mathrm{Ph}]) \tag{A.14}$$

The concentration of the individual species is given by

$$[X_0] = \frac{\lambda_{10}[X_1]}{\lambda_{02} + \Lambda_{05}} = \frac{\lambda_{10}[X_1]}{\lambda_{02} + \lambda_{06}} \tag{A.15}$$

$$[X_1] = \frac{\lambda_{1'1}}{\lambda_{11'}}[\mathrm{TiO_2}] \tag{A.16}$$

$$[X_2] = \frac{\lambda_{2'2}}{\lambda_{22'}}[\mathrm{TiO_2}] \tag{A.17}$$

$$[X_5] = \frac{\lambda_{5'5}}{\lambda_{55'}}[\mathrm{TiO_2}] \tag{A.18}$$

$$[X_3] = \frac{\lambda_{23}}{\lambda_{34}}[X_2] \tag{A.19}$$

$$[X_4] = \frac{\Lambda_{24}}{\lambda_{45}}[X_2] = \frac{\lambda_{23}}{\lambda_{45}}[X_2] \tag{A.20}$$

$$[X_6] = \frac{\lambda_{10}\lambda_{06}[X_1]}{\lambda_{65}(\lambda_{02} + \Lambda_{05})} = \frac{\lambda_{10}\lambda_{06}[X_1]}{\lambda_{65}(\lambda_{02} + \lambda_{06})} \tag{A.21}$$

$$[X_7] = \frac{\lambda_{57}[X_5]}{\lambda_{75} + \lambda_{71}} \tag{A.22}$$

The λ terms in the above equations refer to the pseudo first order reaction rate coefficients given by

$$\lambda_{1'1} = k_{1'1}[D]\,; \quad \lambda_{11'} = k_{11}; \quad \lambda_{10} = k_{10}[h\nu]; \quad \lambda_{02} = k_{02}; \quad \lambda_{21} = k_{21}$$

$$\lambda_{2'2} = k_{2'2}; \quad \lambda_{22'} = k_{22'}$$

$$\lambda_{23} = k_{23}[\mathrm{O_2}]; \quad \lambda_{34} = k_{34}; \quad \lambda_{45} = k_{45}$$

$$\lambda_{06} = k_{06}; \quad \lambda_{65} = k_{65}[\mathrm{O_2}]$$

$$\lambda_{5'5} = k_{5'5}[D]; \quad \lambda_{55'} = k_{55'}$$

$$\lambda_{57} = k_{57}[\mathrm{Ph}]; \quad \lambda_{75} = k_{75}; \quad \lambda_{71} = k_{71} \tag{A.23}$$

After substitution of the Eqs. (A.23) in Eqs. (A.15)–(A.22), Eq. (A.13) is given by

$$[X_T] = [\mathrm{TiO_2}](K_1' + K_2'[\mathrm{D}] + K_3'[\mathrm{D}][\mathrm{Ph}]) \tag{A.24}$$

where the lumped rate coefficients K_1', K_2' and K_3' are given by

$$K_1' = 1 + \frac{k_{2'2}}{k_{22'}} + \frac{k_{23}[\mathrm{O_2}]k_{2'2}}{k_{22'}}\left(\frac{1}{k_{34}} + \frac{1}{k_{45}}\right) \tag{A.25}$$

$$K_2' = \frac{k_{1'1}}{k_{11'}} + \frac{k_{5'5}}{k_{55'}} + \frac{k_{10}[h\nu]k_{1'1}}{(k_{02} + k_{06})k_{11'}}\left(1 + \frac{k_{06}}{k_{65}[\mathrm{O_2}]}\right) \tag{A.26}$$

$$K_3' = \frac{k_{57}k_{5'5}}{(k_{75} + k_{71})k_{55'}} \tag{A.27}$$

The Δ coefficient, according to Eq. (A.12) is given by $\Delta = L_{12}L_{25}L_{51}$. Substitution of the loop coefficients yield

$$\Delta = \left(\frac{k_{10}[h\nu]k_{02}k_{23}[O_2]k_{57}k_{71}}{(k_{02}+k_{06})(k_{75}+k_{71})}\right)[Ph] = K_4'[Ph] \quad (A.28)$$

The D coefficients for the junction nodes X_1, X_2 and X_5 are given by

$$D_{11} = L_{25}L_{51} + L_{21}L_{51} \quad (A.29)$$

$$D_{22} = L_{51}L_{12} \quad (A.30)$$

$$D_{55} = L_{12}L_{25} + L_{15}L_{25} + L_{15}L_{21} \quad (A.31)$$

Substituting the expressions for the loop coefficients and simplification yields

$$D_{11} = \left(k_{23}[O_2]\frac{k_{57}k_{71}}{k_{75}+k_{71}} + k_{21}\frac{k_{57}k_{71}}{k_{75}+k_{71}}\right)[Ph] = K_7'[Ph] \quad (A.32)$$

$$D_{22} = \frac{k_{10}[h\nu]k_{02}k_{57}}{(k_{02}+k_{06})}[Ph] = K_5'[Ph] \quad (A.33)$$

$$D_{55} = \frac{k_{10}[h\nu]}{(k_{02}+k_{06})}(k_{02}k_{23}[O_2] + k_{06}k_{23}[O_2] + k_{06}k_{21}) = K_6' \quad (A.34)$$

The overall D coefficient appearing in the rate expression given by Eq. (A.11) can be written as [11]

$$D = D_{11}\left(1 + \frac{\lambda_{10}}{\lambda_{02}+\Lambda_{05}} + \frac{\lambda_{11'}}{\lambda_{1'1}[D]}\right) + D_{22}\left(1 + C_{23} + C_{24} + \frac{\lambda_{22'}}{\lambda_{2'2}}\right) + D_{55}\left(1 + C_{57} + \frac{\lambda_{55'}}{\lambda_{5'5}[D]}\right) \quad (A.35)$$

where

$$C_{ik} = \frac{\Lambda_{ik}}{\Lambda_{ki}+\Lambda_{kj}} \quad (A.36)$$

Thus

$$D = K_8'[Ph] + K_6' + \frac{K_6''}{[D]} + \frac{K_7''[Ph]}{[D]} \quad (A.37)$$

where

$$K_6'' = K_6'\frac{k_{55'}}{k_{5'5}} \quad (A.38)$$

$$K_7'' = K_7'\frac{k_{11'}}{k_{1'1}} \quad (A.39)$$

$$K_8' = K_7'\left(1 + \frac{k_{10}[h\nu]}{k_{02}+k_{06}}\right) + K_5'\left(1 + \frac{k_{23}[O_2]}{k_{34}} + \frac{k_{23}[O_2]}{k_{45}} + \frac{k_{22'}}{k_{2'2}}\right) + K_6'\frac{k_{57}}{k_{75}+k_{71}} \quad (A.40)$$

Therefore, by substituting the expressions for $[X_T]$, Δ and D, given by Eqs. (A.24), (A.28) and (A.37) in Eq. (A.11) yields

$$r = -\frac{d[Ph]}{dt} = \frac{K_4'[Ph]\left(K_1' + K_2'[D] + K_3'[D][Ph]\right)[TiO_2]}{K_8'[Ph] + K_6' + \frac{K_6''}{[D]} + \frac{K_7''[Ph]}{[D]}} \quad (A.41)$$

As the concentration of the dye and phenolic compounds are low (in ppm (mg L^{-1}) level), the contribution of the cubic and fourth order concentration terms that appear in the above equation, when simplified, is less and hence can be ignored. The final expression after simplification is given by

$$r = -\frac{d[Ph]}{dt} = \frac{[Ph][D][TiO_2]}{K_1^{-1}[Ph][D] + K_2^{-1}[Ph] + K_3^{-1}[D] + K_4^{-1}} \quad (A.42)$$

where K_1, K_2, K_3 and K_4 are given by $K_1'K_4'/K_8'$, $K_1'K_4'/K_7''$, $K_1'K_4'/K_6'$ and $K_1'K_4'/K_6''$, respectively.

Appendix B. Supplementary data

Supplementary data associated with this article can be found, in the online version, at doi:10.1016/j.cej.2010.10.018.

References

[1] J. Zhao, C. Chen, W. Ma, Photocatalytic degradation of organic pollutants under visible light irradiation, Top. Catal. 35 (2005) 269–278.
[2] G. Liu, L. Wang, H.G. Yang, H.-M. Cheng, G.Q. Lu, Titania-based photocatalysts – crystal growth, doping and heterostructuring, J. Mater. Chem. 20 (2010) 831–843.
[3] W.A. Massad, S. Bertolotti, N.A. Garcia, Kinetics and mechanism of the vitamin B_2-sensitized photooxidation of isoproterenol, Photochem. Photobiol. 79 (2004) 428–433.
[4] K. Vinodgopal, D.E. Wynkoop, P.V. Kamat, Environmental photochemistry on semiconductor surfaces: photosensitized degradation of a textile azo dye, acid orange 7, on TiO_2 particles using visible light, Environ. Sci. Technol. 30 (1996) 1660–1666.
[5] C. Zhang, W. Chen, J. Ma, Zhao, Visible-light-induced aerobic oxidation of alcohols in a coupled photocatalytic system of dye-sensitized TiO_2 and TEMPO, Angew. Chem. Int. Ed. 47 (2008) 9730–9733.
[6] M. Yin, Z. Li, J. Kou, Z. Zou, Mechanism investigation of visible light-induced degradation in a heterogeneous TiO_2/Eosin Y/Rhodamine B system, Environ. Sci. Technol. 43 (2009) 8361–8366.
[7] H. Zhang, R. Zong, J. Zhao, Y. Zhu, Dramatic visible photocatalytic degradation performances due to synergetic effect of TiO_2 and PANI, Environ. Sci. Technol. 42 (2008) 3803–3807.
[8] H.-C. Liang, X.-Z. Li, Visible-induced photocatalytic reactivity of polymer sensitized titania nanotube films, Appl. Catal. B: Environ. 86 (2009) 8–17.
[9] D. Zhang, R. Qiu, L. Song, E. Brewer, Y. Mo, X. Huang, Role of oxygen active species in the photocatalytic degradation of phenol using polymer sensitized TiO_2 under visible light irradiation, J. Hazard. Mater. 163 (2009) 843–847.
[10] K. Nagaveni, G. Sivalingam, M.S. Hegde, G. Madras, Solar photocatalytic degradation of dyes: high activity of combustion synthesized nano TiO_2, Appl. Catal. B: Environ. 48 (2004) 83–93.
[11] T.-S. Chen, J.-M. Chern, General rate equations and their applications for cyclic reaction networks: pyramidal systems, Chem. Eng. Sci. 58 (2003) 1407–1415.
[12] C.-H. Wu, J.-M. Chern, Kinetics of photocatalytic decomposition of methylene blue, Ind. Eng. Chem. Res. 45 (2006) 6450–6457.
[13] R. Vinu, G. Madras, Kinetics of simultaneous photocatalytic degradation of phenolic compounds and reduction of metal ions with nano-TiO_2, Environ. Sci. Technol. 42 (2008) 913–919.
[14] R. Vinu, G. Madras, Kinetics of sonophotocatalytic degradation of anionic dyes with nano-TiO_2, Environ. Sci. Technol. 43 (2009) 473–479.
[15] R. Vinu, G. Madras, Photocatalytic activity of Ag-substituted and impregnated nano-TiO_2, Appl. Catal. A: Gen. 366 (2009) 130–140.
[16] K. Nagaveni, M.S. Hegde, N. Ravishankar, G.N. Subbanna, G. Madras, Synthesis and structure of nanocrystalline TiO_2 with lower band gap showling high photocatalytic activity, Langmuir 20 (2004) 2900–2907.
[17] H.J. Kuhn, S.E. Braslavsky, R. Schmidt, Chemical actinometry, Pure Appl. Chem. 76 (2004) 2105–2146.
[18] W.R. Duncan, O.V. Prezhdo, Theoretical studies of photoinduced electron transfer in dye-sensitized TiO_2, Annu. Rev. Phys. Chem. 58 (2007) 143–184.
[19] J.F. Rabek, Photodegradation of Polymers: Physical Characteristics and Applications, Springer-Verlag, Berlin, 1996.
[20] A. Kathiravan, V. Anbazhagan, M.A. Jhonsi, R. Renganathan, Fluorescence quenching of xanthenes dyes by TiO_2, Z. Phys. Chem. 221 (2007) 941–948.
[21] J. Moser, M. Grätzel, Photosensitized electron injection in colloidal semiconductors, J. Am. Chem. Soc. 106 (1984) 6557–6564.
[22] Z.-S. Wang, K. Sayama, H. Sugihara, Efficient eosin Y dye-sensitized solar cell containing Br^-/Br_3^- electrolyte, J. Phys. Chem. B 109 (2005) 22449–22455.
[23] T. Wu, G. Liu, J. Zhao, H. Hidaka, N. Serpone, Mechanistic study of the TiO_2-assisted photodegradation of squarylium cyanine dye in methanolic suspensions exposed to visible light, New J. Chem. 24 (2000) 93–98.
[24] Z. Zhang, C.-C. Wang, R. Zakaria, J.Y. Ying, Role of particle size in nanocrystalline TiO_2-based photocatalysts, J. Phys. Chem. B 102 (1998) 10871–10878.
[25] G. Sivalingam, M.H. Priya, G. Madras, Kinetics of photodegradation of substituted phenols by solution combustion synthesized TiO_2, Appl. Catal. B: Environ. 51 (2004) 67–76.
[26] P. Górska, A. Zaleska, J. Hupka, Photodegradation of phenol by UV/TiO_2 and Vis/N,C-TiO_2 processes: comparative mechanistic and kinetic studies, Sep. Purif. Technol. 68 (2009) 90–96.
[27] X. Li, J.W. Cubbage, W.S. Jenks, Photocatalytic degradation of 4-chlorophenol. 2. The 4-chlorocatechol pathway, J. Org. Chem. 64 (1999) 8525–8536.
[28] X. Li, J.W. Cubbage, T.A. Tetzlaff, W.S. Jenks, Photocatalytic degradation of 4-chlorophenol. 2. The hydroquinone pathway, J. Org. Chem. 64 (1999) 8509–8524.

[29] Y. Cheng, H. Sun, W. Jin, N. Xu, Photocatalytic degradation of 4-chlorophenol with combustion synthesized TiO_2 under visible light irradiation, Chem. Eng. J. 128 (2007) 127–133.
[30] F. Zhang, J. Zhao, T. Shen, H. Hidaka, E. Pelizzetti, N. Serpone, TiO_2 assisted photodegradation of dye pollutants. II. Adsorption and degradation kinetics of eosin in TiO_2 dispersions under visible light irradiation, Appl. Catal. B: Environ. 15 (1998) 147–156.
[31] M.S. Dieckmann, K.A. Gray, A comparison of the degradation of 4-nitrophenol via direct and sensitized photocatalysis in TiO_2 slurries, Water Res. 30 (1996) 1169–1183.